Crystal Structures of Dipeptides Containing the Dmt-Tic Pharmacophore

Sharon D. Bryant,*,[†] Clifford George,[‡] Judith L. Flippen-Anderson,[‡] Jeffrey R. Deschamps,[‡] Severo Salvadori,[§] Gianfranco Balboni,[||] Remo Guerrini,[§] and Lawrence H. Lazarus[†]

Peptide Neurochemistry, LCBRA, National Institute of Environmental Health Sciences, P.O. Box 12233, Mail Drop C3-04, Research Triangle Park, North Carolina 27709, Naval Research Laboratory, Washington, D.C., Faculty of Pharmaceutical Science and Biotechnology Center, University of Ferrara, I-44100 Ferrara, Italy, and Department of Toxicology, University of Cagliary, I09126 Cagliary, Italy

The crystal structures of three analogues of the potent δ-opioid receptor antagonist H-Dmt-Tic-OH (2′,6′-dimethyl-L-tyrosine-L-1,2,3,4-tetrahydroisoquinoline-3-carboxylate), N,N(CH$_3$)$_2$-Dmt-Tic-OH (**1**), H-Dmt-Tic-NH-1-adamantane (**2**), and N,N(CH$_3$)$_2$-Dmt-Tic-NH-1-adamantane (**3**) were determined by X-ray single-crystal analysis. Crystals of **1** were grown by slow evaporation, while those of **2** and **3** were grown by vapor diffusion. Compounds **1** and **3** crystallized in the monoclinic space group $P2_1$, and **2** crystallized in the tetragonal space group $P4_3$. Common backbone atom superimpositions of structures derived from X-ray diffraction studies resulted in root-mean-square (rms) deviations of 0.2−0.5 Å, while all-atom superimpositions gave higher rms deviations from 0.8 to 1.2 Å. Intramolecular distances between the aromatic ring centers of Dmt and Tic were 5.1 Å in **1**, 6.3 Å in **2**, and 6.5 Å in **3**. The orientation of the C-terminal substituent 1-adamantane in **2** and **3** was affected by differences in the ψ torsion angles and strong hydrogen bonds with adjacent molecules. Despite the high δ-opioid receptor affinity exhibited by each analogue (K_i < 0.3 nM), high μ-receptor affinity (K_i < 1 nM) was manifested only with the bulky C-terminal 1-adamantane analogues **2** and **3**. Furthermore, the bioactivity of both **2** and **3** exhibited μ-agonism, while **3** also had potent δ-antagonist activity. Those data demonstrated that a C-terminal hydrophobic group was an important determinant for eliciting μ-agonism, whereas N-methylation maintained δ-antagonism. Furthermore, the structural results support the hypothesis that expanded dimensions between aromatic nuclei is important for acquiring μ-agonism.

Introduction

The δ-, κ-, μ-opioid receptors are G-protein coupled molecules located in the central nervous system and in peripheral regions, such as the mouse vas deferens, guinea pig ileum, rabbit jejunum, and the human gastrointestinal tract.[2] These transmembrane receptors and their endogenous ligands (enkephalins,[3] endorphins,[4] dynorphins,[5] and endomorphins[6]) are involved in a number of physiological functions, most notably, nociception, autonomic reflexes, neuroendocrine effects, and thermoregulation.[2] Furthermore, exogenous opioid molecules both naturally occurring and synthetic have been effective in treating a number of human ailments. Morphine has been the drug of choice for treating severe pain,[7] whereas naloxone and naltrexone, among other antagonists, have been utilized to treat alcoholism and narcotic addiction and have reversed the severe side effects of opioid agonists.[8,9] The mechanism of action of opioid ligands is not fully understood. In fact, neither the three-dimensional structures of the opioid receptors nor their ligand binding sites have been determined experimentally. Furthermore, there are only a handful of X-ray structures of potent and receptor-selective opioid ligands. Therefore, the design of new opioid compounds is critical to understanding the opioid system as well as providing leads for new therapeutic compounds exhibiting fewer side effects.

An essential goal in the development of new opioid compounds is the formation of agonists and antagonists with a high degree of selectivity for either one specific receptor subtype or a combination of characteristics that permit the ligand to interact with high affinity at two distinct receptors while eliciting opposite effects as a bi- or heterofunctional molecule.[10−12] The introduction of 2′,6′-dimethyl-L-tyrosine (Dmt) in place of Tyr into δ-opioid antagonists[13,14] and various agonists[15−21] yielded analogues whose affinities for the δ- and μ-opioid receptors increased by orders of magnitude, frequently causing a reversal of the spectrum of their bioactivities.[12,22] Modification of the aromatic ring of Tic,[2,14] substitution by other aromatic nuclei at the second position,[11,23] or a variety of C-terminal substituents in the Dmt-Tic pharmacophore[22,24] caused major disruptions in the accessibility of the peptide to the receptor binding site. Whereas substitutions for the C-terminal carboxylate, such as an amino acid, an amide function[13] or various hydrophobic groups,[22,24] resulted in relatively minor effects on δ-opioid affinities, μ-receptor affinities increased by orders of magnitude. On the other hand, with the exception of N- or N,N-alkylation with methyl groups, which substantially enhanced bioactivity,[25] all other alterations at the N-terminus were detrimental.[14,25]
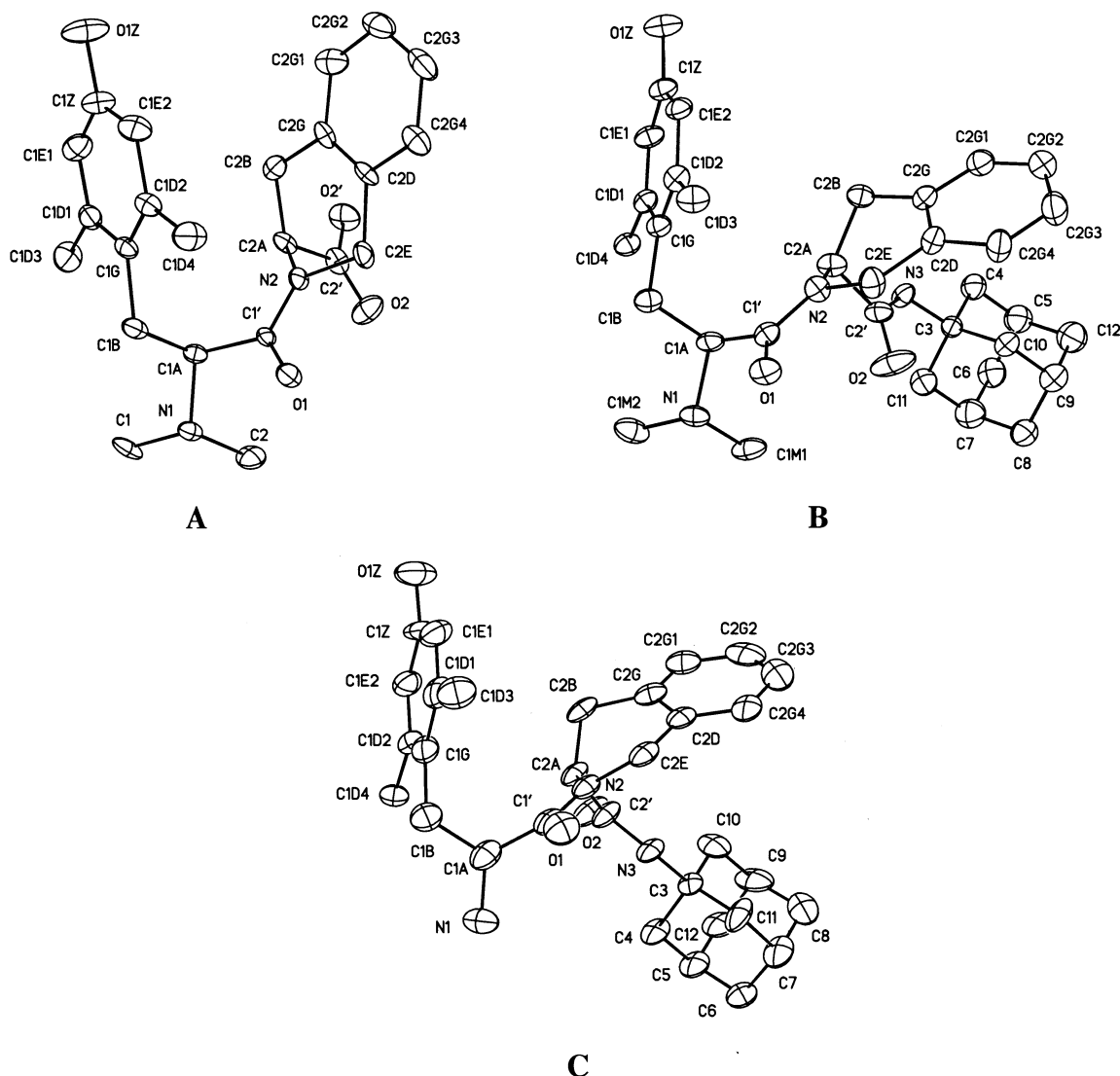
* To whom correspondence should be addressed. Phone: 1-919-541-4962. Fax: 1-919-541-0696. E-mail: bryant2@niehs.nih.gov.
　† National Institute of Environmental Health Sciences.
　‡ Naval Research Laboratory.
　§ University of Ferrara.
　|| University of Cagliary.

Figure 1. X-ray crystal structures of N,N-(CH$_3$)$_2$-Dmt-Tic-OH (A), N,N-(CH$_3$)$_2$-Dmt-Tic-NH-1-adamantane (B), and H-Dmt-Tic-NH-1-adamantane (C) with atom labels. Cl ions, water molecules, lower occupancy disorder, and hydrogen atoms are not displayed.

Although several molecular models were developed for the Dmt-Tic pharmacophore,[26−29] a consensus opinion about the bioactive conformation is lacking despite the similarity between many of the proposed low-energy conformations. In addition, molecular modeling of several Dmt-Tic and Tyr-Tic analogues demonstrated that small changes around Dmt or Tyr did not produce large changes in conformation,[30] and this was noted in the crystal structures of **1**−**3** as presented herein. On the other hand, crystalline parameters for **1**−**3** differed from those obtained from the crystal structures of δ-opioid antagonists TIPP (H-Tyr-Tic-Phe-Phe-OH)[31] and ICI 174,864 and the μ-agonist D-TIPP-NH$_2$.[32] Since molecules **1**−**3** were not crystallized while bound to the receptor, we cannot unequivocally confirm that their crystal-state structures represent bioactive forms. However, we can provide the X-ray crystal coordinates of low-energy forms of conformationally constrained opioids with potent and diverse bioactivities. These data represent the first crystalline structures of potent opioid peptides containing the Dmt-Tic pharmacophore, thereby providing critical starting points for molecular modeling and templates for the design of new therapeutic opioid ligands.

Results and Discussion

The synthesis and biological activity of **1**−**3** were reported previously.[22,25] The X-ray structures of the compounds are represented in Figure 1. Atomic coordinates, bond lengths, bond angles, torsion angles, and anisotropic displacement parameters are available as Supporting Information. The bond distances and angles in all of the structures were at normal values, and a list of selected torsion angles is given in Table 1. The peptide bond between Dmt and Tic in each of the structures was cis, and little variability was noted for values of ω_1, χ^1, and χ^2 of Dmt (Table 1, Figure 2). In contrast, values for ψ_2 of Tic in compounds **2** and **3** varied (Table 1), thereby producing different orientations of the C-terminal carbonyl and adamantyl groups (Figure 2). Backbone superimpositions of structures resulted in root-mean-square (rms) deviations of 0.2−0.5 Å (Figure 2). The small deviations were not surprising because the backbone atom distances C$^\alpha$−C$^\alpha$ and N−C′ and the main-chain torsion angles ϕ, ψ_1, and ω_1 were similar for each compound (Table 1). However, all-atom superimpositions gave larger rms deviations from 0.8 to 1.2 Å (Figure 3). This was explained by the

Table 1. Selected Torsion Angles of X-ray Structures of N,N-(CH$_3$)$_2$-Dmt-Tic-OH (**1**), H-Dmt-Tic-NH-1-adamantane (**2**), and N,N-(CH$_3$)$_2$-Dmt-Tic-NH-1-adamantane (**3**)^a

| compound | residue | angle (deg) | | | | | distance (Å) |
		ϕ	ψ	χ^1	χ^2	ω	
1	Dmt		144.5(7)	−170.5(7)	84.6(10)	−20.3(12)	5.1
	Tic	−102.4(9)		42.9(10)	164.4(8)		
2	Dmt		136.2(8)	−178.3(8)	86.4(10)	−1.0(12)	6.3
	Tic	−95.9(9)	−13.8(11)	63.5(8)	135.9(8)	−169.6(7)	
3	Dmt		142.8(5)	−168.1(5)	85.6(7)	−23.2(8)	6.5
	Tic	−86.8(7)	−170.3(5)	62.3(7)	138.9(6)	168.8(5)	

^{a} Estimated standard deviations appear in parentheses. Distance indicates interatomic distances between aromatic ring centroids of Dmt and Tic.

variability of ψ_2 of **2** and **3** and $\chi_2{}^1$ and $\chi_2{}^2$ of **1** in contrast to those of **2** and **3** (Table 1). Interatomic distances between the aromatic ring centroids of Dmt and Tic varied with values of 5.1 Å in **1**, 6.3 Å in **2**, and 6.5 Å in **3**. The variability in Tic aromatic ring orientations was most prominent between **1** and **2** and between **1** and **3**, while the aromatic groups of **2** and **3** were more closely aligned (Figure 2, Table 1).

Interestingly, crystal structures of chemically similar dipeptides, such as H-Tyr-Tic-OH and H-Tyr-Tic-NH$_2$, had conformations similar to **1** while the positions of the Tic aromatic rings differed from those in **2** and **3**.[33] In contrast, crystal structures of TIPP analogues shared spatial orientations with **2** and **3** because of the C-terminal adamantyl extensions and the χ^2 values of Tic. C-terminal substitutions of the Dmt-Tic/Tyr-Tic pharmacophores may influence orientations of the aromatic ring of Tic during packing of the crystal. The dipeptides appear to favor a stacked conformation of Dmt relative to Tic with a minimum distance between aromatic centers (e.g., **1**),[28] which differs from the orientation of Tic in **2** and **3** and the TIPP analogues.[31,32]

Compounds **1** and **3** both crystallized as chloride salts, and hydrogen bonds were observed between the Dmt hydroxyl group (Oz-Hz) and the chloride (Cl) ion (Table 2). This suggested that the hydroxyl group of Dmt could potentially serve as a hydrogen bond donor in receptor binding interactions. This observation is underscored by several studies that demonstrated a complete loss of ligand−receptor interactions with the δ-opioid receptor when the hydroxyl group of the first residue in opioid peptides is absent or modified.[34−36] However, Phe-c[D-Cys-Phe-D-Pen]NH$_2$ retained high μ-receptor affinity (K_i = 1.36 nM) without the tyrosyl function.[36] Nevertheless, the methyl groups at positions 2′ and 6′ of Tyr (Dmt) of these peptides may stabilize the position of the hydroxyl group of Dmt to form optimal hydrogen bonds within the receptor pocket and may account for the enhanced bioactivities of all Dmt containing ligands.[13−20]

Compound **2** contained eight sites for water oxygens of which only two were at full occupancy. In one of the water sites, hydrogen bonds were formed between the water and the N-terminal protons (Table 2). The large number of water molecules present in the crystal suggest that this low-energy conformation could form in aqueous solution, making it an excellent candidate for structure−activity relationship studies. Strong hydrogen bonds, namely, O(1Z)−H(1ZA)···O(2) in **2** and N(3)−H(3N)···O(1) in **3** may account for the different orientations of the adamantyl groups and can also represent potential stabilizing interactions formed within the receptor binding pocket (Figure 2, Table 2).

Comparison of Crystal Structures and Bioactivity. Compound **1**, which lacks the bulky hydrophobic adamantyl substituent and has an aromatic ring distance of 5.1 Å, interacted selectively with the δ-opioid receptor as an antagonist (Tables 1 and 3). Similarly, low-energy models of other δ-opioid antagonists, such as c(Dmt-Tic)[27] and H-Dmt-Tic-OH,[28] featured comparable aromatic ring distances. The δ-opioid antagonist TIPP[31] had aromatic ring distances of 5.9 Å between Tyr and Tic and 4.2 Å between Tic and Phe,[3] while Tyr and Tic appeared aligned as observed in **1**. In fact, superimposition of Dmt-Tic of **1** with the Tyr-Tic portion of TIPP resulted in a 0.59 Å rms deviation. In contrast, none of the aromatic groups were aligned in the crystal structure of D-TIPP, a μ-antagonist.[32] The alignment of aromatic groups as well as the proximity may be defining structural features for δ-antagonists containing the Dmt-Tic or Dmt-aromatic pharmacophores. In contrast, compounds **2** (μ-agonist) and **3** (δ-antagonist/μ-agonist) exhibited aromatic ring distances around 6.5 Å and the rings were not aligned as observed in **1** (Tables 1 and 3, Figure 2). It has been proposed that the μ-opioid receptor pocket requires ligands with extended architectures[37] in which the intramolecular distances between aromatic residues fall in the range of 10−11 Å or greater. These features were observed among several low-energy conformations of the δ-agonist deltorphin.[28,38,39] In fact, centroid ring distances can range considerably in opioid ligands, e.g., 5.0 to 15.9 Å in enkephalins[40−43] and 9.6 to 15.9 Å in DPDPE[44] and JOM-13,[45] depending on the form and conformation studied. The Dmt-Tic distance and aromatic ring orientation may be critical features of the message domain of Dmt-Tic opioid ligands, since it contains the required hydroxyl group on Dmt, whereas residues or substituents at the C terminal of Tic may constitute the address domain.[46] In addition, hydrophobic structural extensions on the Dmt-Tic pharmacophore may be a definitive characteristic for μ-agonism as observed with molecules **2** and **3** (Table 3, Figures 1−3).

Conclusions

The importance of the X-ray crystal structures of three potent opioid ligands containing the Dmt-Tic pharmacophore cannot be overestimated. Single crystals are grown from solutions, and molecules in solution have an energy-dependent distribution where low-energy conformations are the most populated. These low-energy conformers aggregate to form crystals, and if they cannot pack efficiently alone, then they incorporate water or other solvent molecules to fill the voids that would otherwise be left between the molecules.
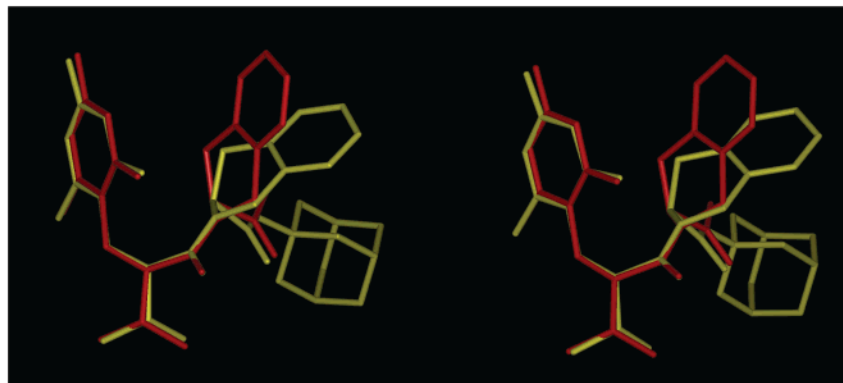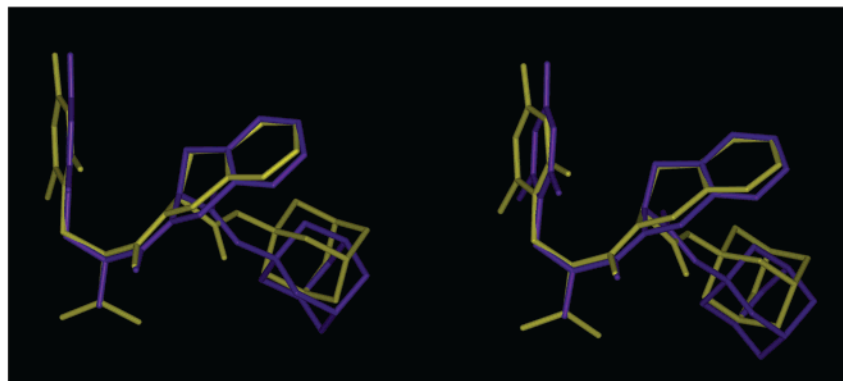
Figure 2. Stereoviews of the backbone superimpositions of (A) N,N-(CH$_3$)$_2$-Dmt-Tic-OH (red) and H-Dmt-Tic-NH-1-adamantane (purple) with rms deviation of 0.2 Å, (B) N,N-(CH$_3$)$_2$-Dmt-Tic-OH (red) and N,N-(CH$_3$)$_2$-Dmt-Tic-NH-1-adamantane (yellow) with rms deviation of 0.2 Å, and (C) H-Dmt-Tic-NH-1-adamantane (purple) and N,N-(CH$_3$)$_2$-Dmt-Tic-NH-1-adamantane (yellow) with rms deviation of 0.5 Å. Hydrogen atoms are not displayed.

Crystal packing forces can affect the peptide conformation formed in the crystalline environment; however, this typically causes only insignificant changes in conformation. In fact, when data have been available to compare X-ray results with modeling results, the conformations determined by X-ray methods matched at least one of the low-energy conformers predicted using molecular modeling techniques. This occurred in comparisons between X-ray structures and models of the enkephalin derivatives, DPDPE,[34,47] JOM-13,[35] and Tyr[1]-c(D-Pen[2]-Gly-Phe[4]-L/D-3-Mpt[5]),[48] as well as other compounds such as D-TIPP-NH$_2$,[23] 1-(2,6-difluorobenzoyl)-5-(4-chlorophenyl)biuret,[49] and molecules **1**−**3** pre-sented here. Therefore, valuable information can be extracted from both modeling and X-ray studies, and agreement between the data derived from different sources reinforces the premises presented.

In addition, crystal packing and intermolecular hydrogen bonding with ions, water molecules, or adjacent Dmt-Tic molecules provide clues about potential receptor binding site interactions and conformations. For example, strong hydrogen bonds between the hydroxyl group of Dmt and a carbonyl group of molecules in the crystal of **2** as well as between an amide hydrogen and a carbonyl of molecules in the crystal of **3** may represent stabilizing hydrogen bond interactions that could form

Figure 3. Stereoview of all-atom superimpositions of N,N-(CH$_3$)$_2$-Dmt-Tic-OH (**1**) (red), H-Dmt-Tic-NH-1-adamantane (**2**) (purple), and N,N-(CH$_3$)$_2$-Dmt-Tic-NH-1-adamantane (**3**) (yellow). The rms deviation between **1** and **2** was 0.8 Å, and the rms deviation between **1** and **3** as well as that between **2** and **3** were 1.2 Å. Hydrogen atoms are not displayed.

Table 2. Hydrogen Bonds for N,N-(CH$_3$)$_2$-Dmt-Tic-OH (**1**), H-Dmt-Tic-NH-1-adamantane (**2**), and N,N-(CH$_3$)$_2$-Dmt-Tic-NH-1-adamantane (**3**)[a]

compound	D−H⋯A	d(D−H)	d(H⋯A)	d(D⋯A)	∠(DHA)
1	O(1Z)−H(1ZA)⋯Cl(1)	0.85(16)	2.55(16)	3.089(9)	122(13)
	N(1)−H(1D)⋯Cl(1)	0.88(10)	2.21(10)	3.071(8)	165(8)
	O(2′)−H(2′)⋯O(1)	0.77(12)	2.00(13)	2.756(9)	165(15)
2	O(1Z)−H(1ZA)⋯O(2)	0.82	1.79	2.606(9)	178
	N(1)−H(1B)⋯O(2S)	0.86	2.47	3.252(14)	152
	N(1)−H(1A)⋯O(1)	0.86	2.29	2.819(10)	120
	O(1S)−H(1SA)⋯O(2S)	0.860(8)	2.39(13)	2.966(11)	124(13)
3	O(1Z)−H(1ZA)⋯Cl(1)	0.96(2)	2.51(5)	2.954(4)	108(3)
	N(1)−H(1A)⋯Cl(1)	0.91	2.32	3.078(5)	141
	N(3)−H(3N)⋯O(1)	1.03(6)	2.02(7)	3.026(7)	164(5)

[a] Distances are reported in Å. Estimated standard deviations appear in parentheses. Symmetry operators are reported in the Supporting Information.

Table 3. Receptor Binding and Bioactivity of Dmt-Tic Analogues

| | receptor binding (K_i, nM) | | bioactivity | | | | | |
| | | | MVD | | | GPI | | |
compound	δ	μ	pA$_2$	K_e (nM)	ED$_{50}$ (μM)	pA$_2$	K_e (μM)	ED$_{50}$ (μM)
1, N,N-(CH$_3$)$_2$-Dmt-Tic-OH	0.12 ± 0.02	2435 ± 462	9.4	0.28	a	5.8	1.58	5.64[b]
2, H-Dmt-Tic-NH-1-adamantane	0.26 ± 0.05	0.76 ± 0.05		>10 000	0.87	a	a	0.036[c]
3, N,N-(CH$_3$)$_2$-Dmt-Tic-NH-1-adamantane	0.16 ± 0.02	1.12 ± 0.10	9.06	0.87	a	a	a	0.016[c]

[a] Absence of activity. [b] Data are from the following: Salvadori, S.; et al. *J. Med. Chem.* **1997**, *40*, 3100. [c] Data are from the following: Salvadori, S.; et al. *J. Med. Chem.* **1999**, *42*, 5010.

within the receptor pocket. In addition, the presence of water in the crystal of **2** suggests that this low-energy conformation might form in solution, making it an excellent candidate for structure−activity investigations.

In general, each of these structures is useful for structure−activity studies because while they are chemically similar, they also exhibit distinct bioactivities allowing us to identify structural components that may be associated with opioid receptor selectivity or bioactivity. The prominent structural differences between **1** and **2** and between **1** and **3** are the ring distances and the C-terminal substitutions. On the basis of the bioactivity and structural data, it can be surmised that increased distances between the aromatic rings of Dmt and Tic and C-terminal hydrophobic substitutions may be structural features associated with μ-agonism, while alignment of the aromatic rings may hinder interactions within the μ-receptor in molecules containing the Dmt-Tic pharmacophore. These hypotheses have been supported by recent evidence demonstrating that C-terminally extended analogues of Dmt-Tic can markedly alter receptor selectivity and reverse functional bioactivity.[12]

Whether three-dimensional structures can be used to predict bioactivities of opioid ligands is debatable and is an area of growing interest. However, X-ray crystallography can provide valuable information regarding potential interaction points of the ligand with the receptor as well as unveil low-energy conformations of similar molecules with distinct bioactivities. In particular, the first crystal-state conformations of opioids containing the Dmt-Tic pharmacophore outlined in this report will contribute to the design of more effective opioid compounds as well as increase our understanding of opioid receptor−ligand interactions.

Experimental Section

Peptide Synthesis. Compounds **1**−**3** were prepared according to previously published standard solution methods.[22,25] Purity was determined to be >99%. The original TFA salt was exchanged for the Cl salt.

Crystallization. Crystals of N,N-(CH$_3$)$_2$-Dmt-Tic-OH (**1**) were grown by slow evaporation from a methanol/2-propanol mixture, while crystals of H-Dmt-Tic-NH-1-adamantane (**2**) and N,N-(CH$_3$)$_2$-Dmt-Tic-NH-1-adamantane (**3**) were grown by vapor diffusion using the hanging drop method.[50,51] A 5 μL drop of a 5.4 mg/mL stock solution of the HCl salt of **2** in 25% acetic

acid was allowed to equilibrate with an equal amount of the reservoir solution over 1 mL of 22% 2-methyl-2,4-pentanediol, 0.5 M LiCl, and 0.1 M sodium acetate (pH 5.0) reservoir solution. Crystals of the free base grew after 3 weeks at 22 °C as a hydrate. Crystals of **3** as the HCl salt were grown from 5 μL of a 4.0 mg/mL methanol stock solution mixed equally with a 22% 2-methyl-2,4-pentanediol, 0.5 M LiCl, and 0.1 M sodium citrate (pH 6.0) reservoir solution. Crystals formed at 22 °C after 2 months, at which time an additional 3 μL of the stock solution of **3** was added to the drop and the crystals were allowed to grow for another fortnight.

Single-Crystal X-ray Diffraction Analysis. N,N-(CH₃)₂-Dmt-Tic-OH: $C_{23}H_{29}N_2{}^+O_4\cdot Cl^-$, FW = 432.93, monoclinic space group $P2_1$, $a = 9.091(1)$ Å, $b = 12.111(1)$ Å, $c = 10.811$-(1) Å, $\beta = 106.89(1)°$, $V = 1102.1(3)$ Å^3, $Z = 2$, $\rho_{calc} = 1.305$ mg mm^{-3}, λ(Cu Kα) = 1.541 78 Å, $\mu = 1.795$ mm^{-1}, $F(000) = 460$, $T = 293$ K.

A clear, colorless 0.38 mm × 0.16 mm × 0.06 mm crystal was used for data collection on an automated Bruker P4 diffractometer equipped with an incident beam monochromator. Lattice parameters were determined from 53 centered reflections within $11.6 < 2\theta < 50°$. The data collection range had a $\{(\sin \theta)/\lambda\}_{max} = 0.54$. Three standards, monitored after every 97 reflections, exhibited random variations with deviations up to 1.6% during the data collection. A set of 2183 reflections was collected in the $\theta/2\theta$ scan mode, and the ω scan rate (a function of count rate) varied from 5.0 to 30.0 deg/min. There were 1697 unique reflections. Corrections were applied for Lorentz, polarization, and absorption effects. The structure was solved with SHELXTL[52] and refined with the aid of the SHELX97 system of programs. The full-matrix least-squares refinement on F^2 varied 280 parameters: atom coordinates and anisotropic thermal parameters for all non-H atoms. H atoms were included using a riding model [coordinate shifts of C applied to attached H atoms, C—H distances set to 0.93—0.96 Å, H angles idealized, U_{iso}(H) were set to $(1.2-1.5)U_{eq}$(C)]. Final residuals were R1 = 0.066 for the 1307 observed data with $F_o > 4\sigma(F_o)$ and 0.090 for all data. Final difference Fourier excursions gave 0.31 and −0.30 e Å^{-3}.

H-Dmt-Tic-NH-1-adamantane: $C_{31}H_{38}N_3O_3\cdot 5.06(H_2O)$, FW = 590.72, tetragonal space group $P4_3$, $a = 17.224(1)$ Å, $b = 17.224(1)$ Å, $c = 10.751(1)$ Å, $V = 3189.5(5)$ Å^3, $Z = 4$, $\rho_{calc} = 1.218$ mg mm^{-3}, λ(Cu Kα) = 1.541 78 Å, $\mu = 0.723$ mm^{-1}, $F(000) = 1252$, $T = 220$ K.

A clear, colorless 0.58 mm × 0.07 mm × 0.07 mm crystal was used for data collection with a Bruker SMART[4] 1K CCD detector on a Platform goniometer. The Rigaku rotating Cu anode source was equipped with incident beam Göbel mirrors. Lattice parameters were determined using SAINT[53] from 267 centered reflections within $12° < 2\theta < 73°$. The data collection range had a $\{(\sin \theta)/\lambda\}_{max} = 0.54$. A set of 10 457 reflections were collected in the ω scan mode. There were 3375 unique reflections. Corrections were applied for Lorentz, polarization, and absorption effects. The structure was solved with SHELX-TL[52] and refined with the aid of the SHELX97 system of programs. The full-matrix least-squares refinement on F^2 used 37 restraints and varied 420 parameters: atom coordinates and anisotropic thermal parameters for all non-H atoms. H atoms were included using a riding model [coordinate shifts of C applied to attached H atoms, C—H distances set to 0.93—0.96 Å, H angles idealized, U_{iso}(H) were set to $(1.2-1.5)U_{eq}$-(C)]. Final residuals were R1 = 0.086 for the 2622 observed data with $F_o > 4\sigma(F_o)$ and 0.104 for all data. Final difference Fourier excursions gave 0.33 and −0.16 e Å^{-3}. In **2** there are eight sites for disordered water oxygens of which two are at full occupancy. The occupation parameter sums to about 3.0 over the remaining five sites, and hydrogen atoms were included for only the two full-occupancy sites. Additional sites for the waters are possible but not resolvable.

(N,N-(CH₃)₂-Dmt-Tic-NH-1-adamantane: $C_{33}H_{44}N_3O_3\cdot Cl^-$, FW = 566.16, monoclinic space group $P2_1$, $a = 10.204(2)$ Å, $b = 6.883(1)$ Å, $c = 21.417(1)$ Å, $\beta = 102.67(1)°$, $V = 1467.6(1)$ Å^3, $Z = 2$, $\rho_{calc} = 1.322$ mg mm^{-3}, λ(Cu Kα) = 1.541 78 Å, $\mu = 1.500$ mm^{-1}, $F(000) = 608$, $T = 220$ K.

A clear, colorless 0.58 mm × 0.03 mm × 0.03 mm crystal was used for data collection with a Bruker SMART[4] 6K CCD detector on a Platform goniometer. The Rigaku rotating Cu anode source was equipped with incident beam Göbel mirrors. Lattice parameters were determined using SAINT[52] from 2047 centered reflections within $8.5° < 2\theta < 103°$. The data collection range had a $\{(\sin \theta)/\lambda\}_{max} = 0.54$. A set of 4763 reflections were collected in the ω scan mode. There were 2823 unique reflections. Corrections were applied for Lorentz, polarization, and absorption effects. The structure was solved with SHELXTL[52] and refined with the aid of the SHELX97 system of programs. The full-matrix least-squares refinement on F^2 used 101 restraints and varied 407 parameters: atom coordinates and anisotropic thermal parameters for all non-H atoms. H atoms were included using a riding model [coordinate shifts of C applied to attached H atoms, C—H distances set to 0.93—0.96 Å, H angles idealized, U_{iso}(H) set to $(1.2-1.5)U_{eq}$-(C)]. Final residuals were R1 = 0.055 for the 2038 observed data with $F_o > 4\sigma(F_o)$ and 0.078 for all data. Final difference Fourier excursions were 0.23 and −0.19 e Å^{-3}. In **3**, the adamantane moiety is disordered over two sites at occupancies of 55:45. The proximity of the atom positions among these two sites necessitated a number of restraints on the adamantane geometry.

Supporting Information Available: Crystal data, atomic coordinates, and equivalent isotropic displacement parameters, anisotropic displacement parameters, bond lengths and angles, torsion angles, hydrogen coordinates, isotropic displacement parameters, and observed hydrogen bonds for each of the three compounds. This material is available free of charge via the Internet at http://pubs.acs.org. In addition, tables of coordinates, bond distances, bond angles, and anisotropic thermal parameters have been deposited with the Crystallographic Data Centre, Cambridge, CB2, 1EW, England.

References

(1) Symbols and abbreviations are compliant with the recommendations made by the IUPAC-IUB Commission of Nomenclature (*J. Biol. Chem.* **1972**, *247*, 977). Other abbreviations: Dmt, 2′,6′-dimethyl-L-tyrosine; Tic, 1,2,3,4-tetrahydro-3-isoquinoline-3-carboxylic acid; Boc, *tert*-butyloxycarbonyl; DAGO, H-Tyr-D-Ala-Gly-*N*-methyl-Phe-Gly-CH₂OH; *t*Bu, *tert*-butyl; DIPCI, 1,3-diisopropylcarbodiimide; DPDPE, [D-Pen²,⁵]enkephalin, H-Tyr-[D-Pen-Gly-Phe-D-Pen]-OH; JOM-13, Tyr-*c*[D-Cys-Phe-D-Pen]OH; O*t*Bu, *tert*-butyl ester; Fmoc, 9-fluoroenylmethyloxycarbonyl; GPI, guinea pig ileum; MVD, mouse vas deferens; HOBt, 1-hydroxybenzotriazole; Pen, β,β-dimethylcysteine; TIPP, H-Tyr-Tic-Phe-Phe-OH.

(2) Atweh, S. F.; Kuhar, M. J. Distribution and physiological significance of opioid receptors in the brain. *Br. Med. Bull.* **1983**, *39*, 57−59.

(3) Hughes, J.; Smith, T. W.; Kosterlitz, H. W.; Fothergill, L. A.; Morgan, B. A.; Morris, H. R. Identification of two related pentapeptides from the brain with potent opiate agonist activity. *Nature* **1975**, *258*, 577−580.

(4) Li, C. H.; Chung, D. Isolation and structure of an untriakontapeptide with opiate activity from camel pituitary glands. *Proc. Natl. Acad. Sci. U.S.A.* **1976**, *73*, 1145−1148.

(5) Goldstein, A.; Tachibana, S.; Lowney, L. H.; Hunkapiller, M.; Hood, L. Dynorphin-(1−13), an extraordinary potent opioid peptide. *Proc. Natl. Acad. Sci. U.S.A.* **1979**, *76*, 6666−6670.

(6) Zadina, J. E.; Hackler, L.; Gee, L. J.; Kastin, A. J. A potent and selective endogenous agonist for the mu-opiate receptor. *Nature* **1997**, *386*, 499−502.

(7) Mercadante, S.; Villari, P.; Ferrera, P.; Casuccio, A.; Fulfaro, F. Rapid titration with intravenous morphine for severe cancer pain and immediate oral conversion. *Cancer* **2002**, *95*, 203−208.

(8) Kelly, A. M.; Koutsogiannis, Z. Intranasal naloxone for life threatening opioid toxicity. *Emerg. Med. J.* **2002**, *19*, 375.

(9) Gowing, L.; Ali, R.; White, J. Opioid antagonists with minimal sedation for opioid withdrawal. *Cochrane Database Syst. Rev.* **2002**, *2*, CD001333.

(10) Balboni, G.; Salvadori, S.; Guerrini, R.; Bianchi, C.; Santagada, V.; Calliendo, G.; Bryant, S. D.; Lazarus, L. H. Opioid pseudopeptides containing heteroaromatic or heteroaliphatic nuclei. *Peptides* **2000**, *21*, 1663−1671.

(11) Santagada, V.; Balboni, G.; Caliendo, G.; Guerrini, R.; Salvadori, S.; Bianchi, C.; Bryant, S. D.; Lazarus, L. H. Assessment of substitution in the second pharmacophore of Dmt-Tic analogues. *Bioorg. Med. Chem. Lett.* **2000**, *10*, 2745−2748.

(12) Balboni, G.; Guerrini, R.; Salvadori, S.; Bianchi, C.; Rizzi, D.; Bryant, S. D.; Lazarus, L. H. Evaluation of the Dmt-Tic pharmacophore: conversion of a potent δ-opioid receptor antagonist into a potent δ-agonist and ligands with mixed properties. *J. Med. Chem.* **2002**, *45*, 713−720.

(13) Salvadori, S.; Attila, M.; Balboni, G.; Bianchi, C.; Bryant, S. D.; Crescenzi, O.; Guerrini, R.; Picone, D.; Tancredi, T.; Temussi, P. A.; Lazarus, L. H. δ Opioidmimetic antagonists: prototypes for designing a new generation of ultraselective opioid peptides. *Mol. Med.* **1995**, *1*, 678−689.

(14) Lazarus, L. H.; Bryant, S. D.; Cooper, P. S.; Guerrini, R.; Balboni, G.; Salvadori, S. Design of δ-opioid peptide antagonists for emerging drug applications. *Drug Discovery Today* **1998**, *3*, 284−294.

(15) Chandrakumar, N. S.; Yonan, P. K.; Stapelfeld, A.; Savage, M.; Rorbacher, E.; Contreras, P. C.; Hammond, D. Preparation and opioid activity of analogues of the analgesic dipeptide 2,6-dimethyl-L-tyrosyl-*N*-(3-phenylpropyl)-D-alaninamide. *J. Med. Chem.* **1992**, *35*, 223−233.

(16) Hansen, J. D. W.; Stapelfeld, A.; Savage, M. A.; Reichman, M.; Hammond, D. L.; Haaseth, R. C.; Mosberg, H. I. Systemic analgesic activity and δ-opioid selectivity in [2,6-dimethyl-Tyr¹,D-Pen²,D-Pen⁵]enkephalin. *J. Med. Chem.* **1992**, *35*, 684−687.

(17) Pitzele, B. S.; Hamilton, R. W.; Kudla, K. D.; Tsymbalov, S.; Stapelfeld, A.; Savage, M. A.; Clare, M.; Hammond, D. L.; Hansen, J. D. W. Enkephalin analogs as systematically active antinociceptive agents: O- and N-alkylated derivatives of the dipeptide amide L-2,6-dimethyltyrosyl-*N*-(3-phenylpropyl)-D-alaninamide. *J. Med. Chem.* **1994**, *37*, 888−896.

(18) Guerrini, R.; Capasso, A.; Sorrentino, L.; Anacardio, R.; Bryant, S. D.; Lazarus, L. H.; Attila, M.; Salvadori, S. Opioid receptor selectivity alteration by single residue replacement: synthesis and activity profile of [Dmt¹]deltorphin B. *Eur. J. Pharmacol.* **1996**, *302*, 37−42.

(19) Guerrini, R.; Capasso, A.; Marastoni, A.; Bryant, S. D.; Cooper, P. S.; Lazarus, L. H.; Temussi, P. A.; Salvadori, S. Rational design of dynorphin A analogues with δ-receptor selectivity and antagonism for δ- and κ-receptors. *Bioorg. Med. Chem.* **1998**, *6*, 57−62.

(20) Sasaki, Y.; Suto, T.; Ambo, A.; Ouchi, H.; Yamamoto, Y. Biological properties of opioid peptides replacing Tyr at position 1 by 2,6-dimethyl-Tyr. *Chem. Pharm. Bull.* **1999**, *47*, 1506−1507.

(21) Schiller, P. W.; Nguyen, T. M.-D.; Berezowska, I.; Dupuis, S.; Weltrowska, G.; Chung, N. N.; Lemieux, C. Synthesis and in vitro opioid activity profiles of DALDA analogues. *Eur. J. Med. Chem.* **2000**, *35*, 895−901.

(22) Salvadori, S.; Guerrini, R.; Balboni, G.; Bianchi, C.; Bryant, S. D.; Cooper, P. S.; Lazarus, L. H. Further studies on the Dmt-Tic pharmacophore: Hydrophobic substituents at the C-terminus endows δ antagonists to manifest μ agonism or μ antagonism. *J. Med. Chem.* **1999**, *42*, 5010−5019.

(23) Page, D.; McClory, A.; Mischki, T.; Schmidt, R.; Butterworth, J.; St-Onge, S.; Labarre, M.; Payza, K.; Brown, W. Novel Dmt-Tic dipeptide analogues as selective delta-opioid receptor antagonists. *Bioorg. Med. Chem. Lett.* **2000**, *10*, 167−170.

(24) Page, D.; Naismith, A.; Schmidt, R.; Coupal, M.; Labarre, M.; Gosselin, M.; Bellemare, D.; Payza, K.; Brown, W. Novel C-terminus modifications of the Dmt-Tic motif: a new class of dipeptide analogues showing altered pharmacological profiles toward the opioid receptors. *J. Med. Chem.* **2001**, *44*, 2387−2390.

(25) Salvadori, S.; Balboni, G.; Guerrini, R.; Tomatis, R.; Bianchi, C.; Bryant, S. D.; Cooper, P. S.; Lazarus, L. H. Evolution of the Dmt-Tic pharmacophore: N-terminal methylated derivatives with extraordinary δ opioid antagonist activity. *J. Med. Chem.* **1997**, *40*, 3100−3108.

(26) Crescenzi, O.; Fraternali, F.; Picone, D.; Tancredi, T.; Balboni, G.; Guerrini, R.; Lazarus, L. H.; Salvadori, S.; Temussi, P. A. Design and solution structure of a partially rigid opioid antagonist lacking the basic center. *Eur. J. Biochem.* **1997**, *247*, 66−73.

(27) Bryant, S. D.; Balboni, G.; Guerrini, R.; Salvadori, S.; Tomatis, R.; Lazarus, L. H. Opioid diketopiperazines: refinement of the δ opioid antagonist pharmacophore. *Biol. Chem.* **1997**, *378*, 107−114.

(28) Bryant, S. D.; Salvadori, S.; Cooper, P. S.; Lazarus, L. H. New δ opioid antagonists as pharmacological probes. *Trends Pharmacol. Sci.* **1998**, *19*, 42−46.

(29) Santagada, V.; Caliendo, G.; Severino, B.; Perissutti, E.; Ceccarelli, F.; Giusti, L.; Mazzoni, R.; Salvadori, S.; Temussi, P. A. Probing the shape of a hydrophobic pocket in the active site of δ-opioid antagonists. *J. Pept. Sci.* **2001**, *7*, 374−385.

(30) Spadaccini, R.; Temussi, P. A. Natural peptide analgesics: the role of solution conformation. *Cell. Mol. Life Sci.* **2001**, *58*, 1572−1582.

(31) Flippen-Anderson, J. L.; George, C.; Deschamps, J. R.; Reddy, P. A.; Lewin, A. H.; Brine, G. A. X-Ray structures of the δ opioid antagonist TIPP and a protected derivative of the δ antagonist ICI 174,864. *Lett. Pept. Sci.* **1994**, *1*, 107−115.

(32) Flippen-Anderson, J. L.; Deschamps, J. R.; George, C.; Reddy, P. A.; Lewin, A. H.; Brine, G. A.; Sheldrick, G.; Nikiforovich, G. X-Ray structure of Tyr-D-Tic-Phe-Phe-NH₂ (D-TIPP-NH₂), a highly potent μ-receptor selective opioid agonist. *J. Pept. Res.* **1997**, *49*, 384−393.

(33) Deschamps, J. R.; Flippen-Anderson, J. L.; Moore, C.; Cudney, R.; George, C. Tyrosinium-D-tetrahydroisoquinoline-3-carboxylate 1,5-hydrate and tyrosyl-D-tetrahydroisoquinoline-3-carboxamide hydrate. *Acta Crystallogr. C* **1997**, *C53*, 1478−1482.

(34) Schmidt, R.; Menard, D.; Mrestani-Klaus, C.; Chung, N. N.; Lemieux, C.; Schiller, P. W. Structural modifications of the N-terminal tetrapeptide segment of [D-Ala²]deltorphin I: effects on opioid receptor affinities and activities in vitro and on antinociceptive potency. *Peptides* **1997**, *18*, 1615−1621.

(35) Lazarus, L. H.; Bryant, S. D.; Cooper, P. S.; Salvadori, S. What peptides these deltorphins be. *Prog. Neurobiol.* **1999**, *57*, 377−420.

(36) Mosberg, H. I.; Ho, J. C.; Sobczyk-Kojiro, K. A high affinity, mu-opioid receptor-selective enkephalin analogue lacking an N-terminal tyrosine. *Bioorg. Med. Chem. Lett.* **1998**, *8*, 2681−2684.

(37) Goodman, M.; Ro, S.; Osapay, G.; Yamazaki, T.; Polinsky, A. The molecular basis of opioid potency and selectivity: mophiceptins, dermorphins, deltorphins, and enkephalins. *NIDA Res. Monogr.* **1993**, *143*, 195−209.

(38) Bryant, S. D.; Attila, M.; Salvadori, S.; Guerrini, R.; Lazarus, L. H. Molecular dynamics conformations of deltorphin analogues advocate δ opioid binding site models. *Pept. Res.* **1994**, *7*, 175−184.

(39) Bryant, S. D.; Guerrini, R.; Salvadori, S.; Bianchi, C.; Tomatis, R.; Attila, M.; Lazarus, L. H. Helix inducing α-aminoisobutyric acid in opioidmimetic deltorphin C analogues. *J. Med. Chem.* **1997**, *40*, 2579−2587.

(40) Flippen-Anderson, J. L.; Deschamps, J. R.; Ward, K. B.; George, C.; Houghten, R. Crystal structure of deltakephalin: a δ-selective opioid peptide with a novel β-bend-like conformation. *Int. J. Pept. Protein Res.* **1994**, *44*, 97−104.

(41) Aubry, A.; Birlirakis, N.; Sakarellos-Daitsiotis, M.; Sakarellos, C.; Marraud, M. A crystal molecular conformation of leucine-enkephalin related to the morphine molecule. *Biopolymers* **1989**, *28*, 27−40.

(42) Prasad, B. V. V.; Sudha, T. S.; Balaram, P. Molecular structure of Boc-Aib-Aib-Phe-Met-NH₂.DMSO. A fragment of a biologically active enkephalin analogue. *J. Chem. Soc., Perkins Trans.* **1983**, *1*, 417−421.

(43) Stezowski, J. J.; Eckle, E.; Bajusz, S. A crystal structure determination for Tyr-D-Nle-Gly-Phe-NleS [NleS = MeCH₂CH₂-CH₂CH(NH₂)SO₃H]: an active synthetic enkephalin analogue. *J. Chem. Soc.* **1985**, 681−682.

(44) Flippen-Anderson, J.; Hruby, V. J.; Collins, N.; George, C.; Cudney, R. X-ray structure of [D-Pen²,D-Pen⁵] enkephalin, a highly potent, δ opioid receptor-selective compound: comparison with proposed solution conformations. *J. Am. Chem. Soc.* **1994**, *116*, 7523−7531.

(45) Lomize, A.; Flippen-Anderson, J.; George, C.; Mosberg, H. Conformational analysis of the δ receptor-selective, cyclic opioid peptide, Tyr-cyclo[D-Cys-Phe-D-Pen]OH (JOM-13). Comparison of X-ray crystallographic structures, molecular mechanics simulations, and ¹H NMR data. *J. Am. Chem. Soc.* **1994**, *116*, 429−436.

(46) Schwyzer, R. Molecular mechanism of opioid selection. *Biochemistry* **1986**, *25*, 6335−6342.

(47) Collins, N.; Flippen-Anderson, J. L.; Haaseth, R. C.; Deschamps, J. R.; George, C.; Kover, K.; Hruby, V. J. Conformational determinants of agonist versus antagonist properties of [D-Pen²,D-Pen⁵]enkephalin (DPDPE) analogs at opioid receptors. Comparison of X-ray crystallographic structure, solution ¹H NMR data, and molecular dynamic simulations of [L-Ala³]DPDPE and [D-Ala³]DPDPE. *J. Am. Chem. Soc.* **1996**, *118*, 2143−2152.

(48) Nikiforovich, G. V.; Kover, K. E.; Kolodziej, S. A.; Nock, B.; George, C.; Deschamps, J. R.; Flippen-Anderson, J. L.; Marshall, G. R. Design and comprehensive conformational studies of Tyr¹-cyclo(D-Pen²-Gly-Phe⁴-L-3-Mpt⁵) and Tyr¹-cyclo(D-Pen²-Gly-Phe⁴-d-3-Mpt⁵): Novel conformationally constrained opioid peptides. *J. Am. Chem. Soc.* **1996**, *118*, 959−969.

(49) Deschamps, J. R.; George, C.; Flippen-Anderson, J. L.; DeMilo, A. B.; Bordas, B. X-ray crystallographic and molecular modeling studies of 1-(2,6-diflourobenzoyl)-5-(4-chlorophenyl)biuret. *J. Chem. Crystallogr.* **1998**, *28*, 453−459.
(50) McPherson, A. *Preparation and Analysis of Protein Crystals*; John Wiley & Sons: New York, 1982.
(51) Ducruix, A., Girge, R. I., Eds. *Crystallization of Nucleic Acids and Proteins: A Practical Approach*; Oxford University Press: New York, 1992; pp 73−98.

(52) Sheldrick, G. M. *SHELXTL*, version 5.1; Bruker Analytical X-ray Instruments: Madison, WI, 1997.
(53) *Bruker SMART and SAINT Data Collection and Reduction Software for the SMART System*; Bruker-AXS, Bruker Analytical X-ray Instruments: Madison, WI, 1995.